The Journal for Vascular Ultrasound 40(2):70–75, 2016

Ultrasonographic Tissue Characterization of Kidneys in Patients with Unilateral Renal Artery Stenosis

Ana Luiza D. Valiente Engelhorn, MD, MS;[1,2] Carlos A. Engelhorn, MD, PhD;[1,2] Sergio X. Salles-Cunha, PhD, RVT, FSVU;[1] Gabriele Andruska;[2] Karolini Batisti[2]

ABSTRACT *Introduction.*—Ultrasound tissue characterization (USTC) has been applied to B-mode images of normal, young and transplanted kidneys, carotid, and peripheral atherosclerosis and venous thrombosis. We analyzed USTC from both kidneys of patients with severe unilateral renal artery stenosis. Seven women and 11 men, 79 ± 9 standard deviation (range = 57–96) years of age, were included. Severe, unilateral, renal artery stenosis was based on renal artery peak-systolic velocity (PSV) > 200 cm/sec and/or renal-aortic PSV ratio > 3.5. This sample population, selected sequentially by date of ultrasonographic examinations requested, was heterogeneous: kidney lengths and resistivity indices varied from 6.7 to 13.4 cm and 0.45 to 0.85.

Methods.—USTC was applied to images selected for kidney length measurements. Pixel brightness in the 0–255 range was rescaled to zero for black and 200 for fascia brightness. Gray-scale medians (GSM) of entire kidneys were estimated for statistical comparisons between: (a) kidneys ipsilateral to stenosis (KIS), (b) kidneys contralateral to stenosis (KCS), and (c) normal, young kidneys (KN), previously published GSM = 37 ± 6 (27–48).

Results.—Two distinct KCS subgroups were identified: (1) near-normal GSM < 54 (KCSN, n = 10, 56%); and (2) elevated GSM > 60 (KCSH, n = 8, 44%). Subgroup increasing GSM order was (1) KN, (2) KCSN (47 ± 7, > KN, $p < 0.002$), (3) KIS-CN (59 ± 20, >KCSN, $p < 0.003$), (4) KIS-CH (73 ± 20, > KCSN, $p < 0.007$), and (5) KCSH (78 ± 17, >KIS-CN, $p < 0.05$). GSM was independent of kidney length or resistivity index, with Pearson correlation coefficients < 0.5 for either KIS or KCS, respectively.

Conclusions.—Tissue echogenicity, represented by GSM, was an independent variable characterizing effects of unilateral renal artery stenosis on the ipsilateral or on both kidneys.

Introduction

Ultrasonographic tissue characterization (USTC) performed with transcutaneous transducers is an extension of virtual histology (USVH) studies using intravascular ultrasound.[1–13] USTC is also a subset of image tissue characterization (IMTC), a technique applicable to most imaging modalities, including photography.[14,15] USTC and IMTC allow for qualitative and quantitative analyses. USTC was designed to (a) enhance visual perception by artificial colorization and (b) quantitate data based on distributions of image pixels in specific amplitude ranges. A simplified approach reports the gray-scale median (GSM) of the image selected.

Transcutaneous USTC has been applied to US images of normal, young kidneys,[2] transplanted kidneys,[1,16] peripheral and pelvic venous thrombosis,[6–8,17,18] carotid and peripheral artery atheromas,[3,4,9–13] aneurysms,[5] lungs—echogenicity on echocardiography increased with patient hyper hydration (Costa Lima JR, unpublished data), edemas,[19–21] and leg tissue post saphenous vein treatment.[22] We have applied IMTC to (a) thermographic images of subclavian vein thrombosis, peripheral neuropathic ischemia, and ulnar nerve compression syndrome[23–25] and (b) photographic images of venous and diabetic foot ulcers.[14,15]

Working hypotheses for the IMTC-USTC approaches are (a) the human visual system is weak to detect all the information available in medical images[26]; (b) tissue changes may be detectable by US or other imaging modality before symptoms or hemodynamic changes become noticeable[1]; and (c) imaging quantification may be used to follow patient evolution in disease and posttreatment.[20]

This discovery level research focused on kidney disease. This particular application related to echogenicity

From [1]Angiolab, Inc., Noninvasive Vascular Laboratory, Curitiba, Parana, Brazil; and [2]Pontificia Universidade Católica do Paraná, Curitiba, Parana, Brazil.

Accreditation Statement: This activity has been planned and implemented in accordance with the Essential Areas and policies of the Accreditation Council for Continuing Medical Education through the joint sponsorship of the University of Cincinnati and the Society for Vascular Ultrasound. The University of Cincinnati is accredited by the ACCME to provide continuing medical education for physicians. The University of Cincinnati designates this journal activity for a maximum of 1 *AMA PRA Category 1 Credit(s)*™. Physicians should claim only the credits commensurate with the extent of their participation in the activity.

Address correspondence to: Carlos A. Engelhorn, MD, PhD, Angiolab Curitiba, Inc., Rua da Paz, 195, Sala 2, Alto da XV, Curitiba, PR, Brazil CEP 80060-160. E-mails: carlos.engelhorn@pucpr.br or sergioxsc@yahoo.com

of both kidneys in patients with unilateral renal artery stenosis. Direct ischemia may affect the ipsilateral kidney. Systemic changes such as hypertension caused by a deteriorating kidney may also affect the contralateral organ. Therefore, broad alterations affecting the GSM of both kidneys were investigated.

Materials and Methods

Kidney ultrasonography (US) examinations were performed at an International Standard Organization–certified laboratory, Angiolab-Curitiba, Brazil. This project was approved by the Ethics Research Committee of Pontificia Universidade Catolica do Paraná.

This session describes basic renal ultrasonography (US), kidney US tissue characterization, and descriptive and comparative statistics. The primary null hypothesis tested in a population with unilateral renal artery stenosis was that there was no difference in GSM among the kidneys ipsilateral to stenosis (KIS) and contralateral to stenosis (KCS).

Inclusion Criterion

Examination data were collected and stored prospectively. Patients were selected retrospectively once the working hypothesis was established. Patients with unilateral renal artery stenosis were selected sequentially until n = 20.

Exclusion Criteria

Two children, who were sequentially included in the sample population, were excluded from final adult group analysis.

A 9-year-old boy had KCS GSM = 21 and KIS GSM = 29. The kidneys were equal in length at 9.0 cm. A 5-year-old boy had KCS GSM = KIS GSM = 47. The KIS kidney had a greater length than the KCS kidney: 10.0 versus 9.1 cm.

Ultrasonography

Standard renal artery and kidney ultrasonography (US) was performed bilaterally by an experienced, vascular–US certified physician in Brazil.[27,28] A Siemens Antares (Issaquah, WA) instrument was used. Images were obtained with a curved-array 2- to 6-MHz probe. Common indications as hypertension and other causes of renal failure[29] were not analyzed as part of this project. US examinations were commonly performed in the morning after 12-h fasting, in an out-patient setting, and preparation as appropriate for each patient, especially those with large body mass indices.[30] B-mode, color flow, and duplex Doppler data were collected. Essential images described the anatomy and blood flow characteristics of the abdominal aorta, the renal arteries, and the kidneys. Sub or transhepatic, transgastric, transduodenal, transcaval, and trans or pararenal windows were commonly used.[31]

B-mode imaging provided kidney dimensions, in particular, maximum kidney length. The image with maximum kidney length was used for tissue characterization analysis. B-mode and color flow imaging pinpointed renal artery lumen and atheroma's, and mapped flow velocity distribution.

Duplex Doppler provided peak-systolic velocity (PSV) and end-diastolic velocity (EDV) measured (a) at the aorta proximal and distal to renal artery branching, (b) throughout the extent of each renal artery, and (c) at several locations of each kidney: cortex, medulla, pelvis, and hilus. A renal/aorta peak-velocity ratio (RAR) was calculated based on the maximum renal artery velocity and aortic velocity proximal to the renal artery. Resistivity indices (RI) were calculated for the various velocities measured in the renal artery and within the kidney as the systolic–diastolic velocity difference divided by the maximum systolic velocity. RI estimates were preferred over its inverse, the EDV/PSV ratio.[32] A relatively low diastolic flow velocity would result in a high resistivity index.

Inclusion in the analysis was based on reading interpretation of severe unilateral renal artery stenosis. Laboratory guidelines summarized renal artery findings as (a) normal lumen, (b) nonhemodynamic significant stenosis, (c) moderate stenosis, (d) hemodynamically significant stenosis ≥ 60% diameter reduction, or (e) occlusion. Velocity criteria included primarily PSV and RAR. Original PSV = 180 cm/sec was increased to 200 cm/sec based on internal quality control validation and other literature data.[28,33–36] Recent tendency was to use a decision interval 200–250 cm/sec for PSV in association with other information.[35,37] The decision interval for RAR evolved to 3.3–3.5.[28,35] Velocity measurements were correlated with other information such as aortic and renal flow patterns,[38] anatomic imaging of the obstruction, renal artery diameter, tortuosity, and poststenotic turbulence showing disturbed or distorted flow pattern. Kidney length and velocity data were used as secondary variables for questioning renal artery stenosis.[39–41]

Ultrasonographic Tissue Characterization

USTC was restricted to GSM comparisons. GSM was calculated by a software specifically designed for USTC. This program has been successfully tested and applied to a variety of analyses since 2006.[1–8,14–21] This software allows rescale and definitions of variable brightness intervals. Qualitative analysis is obtained using artificial colorization to strike the human visual system; quantitative analysis is based on percentage of pixel in each defined brightness interval.

The image selected to perform kidney maximum length measurement was used for USTC. The kidney image pixels had brightness amplitudes from 0 to 255. All pixel brightness were adjusted to a new 0–200 scale. The objective of rescaling was normalization of distinct image brightness amplitudes affected by gain or tissue attenuation. The new zero was obtained from the black region of the image, away from the kidney ultrasonographic region. The new 200 brightness level was selected from a white-like fascia within the kidney. Overly saturated white fascia was avoided as reference whenever possible. A low/high fascia brightness selected, increased/decreased to 200, and would increase/decrease

the GSM. Quality assurance testing was performed to rule out possible influence of the scale factor for the new 200 brightness level.

Statistical Comparisons

The intended primary analysis was a simple comparison between GSM of the KIS versus KCS. Initial analysis indicated a large variability in KCS GSM. Therefore, five kidney subgroups were identified and compared:

1. KN: normal, young kidneys, GSM previously reported in the literature.[2]
2. KIS-CN: kidney ipsilateral to stenosis with contralateral kidney having low, normal GSM.
3. KIS-CH: kidney ipsilateral to stenosis with contralateral kidney having abnormally high GSM.
4. KCSN: kidney contralateral to stenosis with low, normal GSM.
5. KCSH: kidney contralateral to stenosis with abnormally high GSM.

Paired t test available with the Excel data file was used to compare KIS to KCS, KIS-CN to KCSN, and KIS-CH to KCSH data. A unicaudal comparison was performed assuming that KIS GSM was expected to be higher than KCS GSM. Unpaired t test was selected for comparisons between subgroup pairs including KN, KIS-CN, KIS-CH, KCSN, and KCSH.

Secondary analysis described correlations or lack of between subgroup GSM and kidney lengths and RI.

Results

This session summarizes patient population data, the rescaling quality control data, the GSM descriptive and comparative statistics, and the secondary analysis relating GSM to kidney length and resistivity index.

Patient Population

Eighteen adults with unilateral renal artery stenosis according to the interpretation of the ultrasonographic examination were included in the analysis; 11 were men and 7 were women, 79 ± 9 (range = 57–96) years of age.

The average kidney length for the 18 adults was lower in the side with renal artery stenosis: 9.8 ± 1.4 (6.7–13.1) versus 10.4 ± 1.1 (8.7–13.4) cm (p = 0.03, unicaudal, paired t test, assuming an expectation KIS < KCS in length; p = 0.06 for bicaudal). KIS was smaller than KCS by more than 1 cm in six patients (KIS < KCS – 1 cm), while KCS < KIS – 1 cm in two patients.

Adult RI were 0.70 ± 0.10 (0.45–0.85) for KIS versus 0.73 ± 0.06 (0.63–0.84) for KCS (p = 0.02, bicaudal paired t test). Six kidneys, 3 KIS and 3 KCS, in 5 patients had RI ≥ 0.8; 13 kidneys, 5 KIS and 8 KCS, in 8 patients had RI ≥ 0.75. Two KIS had RI < 0.60.

Pearson coefficients, –0.02, 0.11 and –0.47, showed weak correlations between kidney length and RI for subgroups KIS + KCS, KIS, and KCS. These measurements, therefore, were relatively independent and may demonstrate distinct conditions or alterations.

USTC Scale

The original value of the new 200 brightness value (141–242) averaged 172 ± 25 standard deviation (SD) for the 36 kidneys. The coefficient of variability, SD/mean, was 0.15. Kidney echogenicity, therefore, was increased by 16%, on average prior to USTC analysis. The Pearson correlation coefficient between kidney GSM and fascia brightness level for the new 200 level was –0.12, suggesting minimal or no correlation. The GSM values, therefore, were validated for this analysis, based on this lack of correlation with rescaling.

Kidney GSM

The GSM of the entire kidney for the 18 adults was higher in the side with renal artery stenosis, KIS GSM = 65 ± 20 (29–98), than in the contralateral kidney, KCS GSM = 61 ± 20 (34–108); the difference was not significantly different by bicaudal or unicaudal paired t tests (p > 0.15). KIS GSM was less than 42 in three cases and in the borderline 51–53 values in three other patients.

Table 1

Ultrasonographic Tissue Characterization of Kidneys from Patients with Hemodynamically Significant Unilateral Renal Artery Stenosis (Gray-scale median [GSM] for Five Subgroups)

Subgroup	Kidney—Renal Artery Stenosis	GSM Mean ± SD	GSM Range
Normal, young kidneys, n = 20	KN no stenosis	37 ± 6	27–48
Near-normal contralateral kidney GSM < 54, n = 10	KCSN contralateral stenosis	47 ± 7	34–53
	KIS-CN ipsilateral stenosis	59 ± 20	29–89
Elevated contralateral kidney GSM > 60, n = 8	KIS-CH ipsilateral stenosis	73 ± 20	41–98
	KCSH contralateral stenosis	78 ± 17	61–108

KN, normal, young kidneys, literature data; KIS, kidney ipslateral to renal artery stenosis; KIS-CN, contralateral kidney with near-normal GSM; KIS-CH, contralateral kidney with high GSM; KCS, kidney contralateral to renal artery stenosis; KCSN, near-normal GSM; KCSH, high GSM. Statistical comparisons between subgroups showed that (a) KCSN GSM > KN GSM, p = 0.001 for unpaired t test, bicaudal, and same variance; (b) KIS-CN GSM > KCSN GSM, p < 0.003 for paired t test, and unicaudal; (c) KIS-CH GSM > KCSN GSM, p < 0.007 for unpaired t test, bicaudal, and uniqual variance; and (d) KCSH GSM > KIS-CN GSM, p < 0.05 for unpaired t test, bicaudal, and same variance.

Further analysis identified two subgroups of KCS based on GSM: (1) KCSN, kidneys contralateral to renal artery stenosis with near-normal GSM < 54 and (2) KCSH, contralateral kidneys with high GSM > 60. KIS to renal artery stenoses were also subdivided in two groups: (1) KIS-CN, ipsilateral kidneys having a contralateral kidney with near-normal GSM and (2) KIS-CH, ipsilateral kidneys having a contralateral kidney with high GSM. Table 1 lists the GSM of these four subgroups in comparison with the GSM of normal, young kidneys as previously reported in the literature. Figure 1 exemplifies USTC applied to extreme cases of patients having (a) high or (b) low echogenicities of both kidneys.

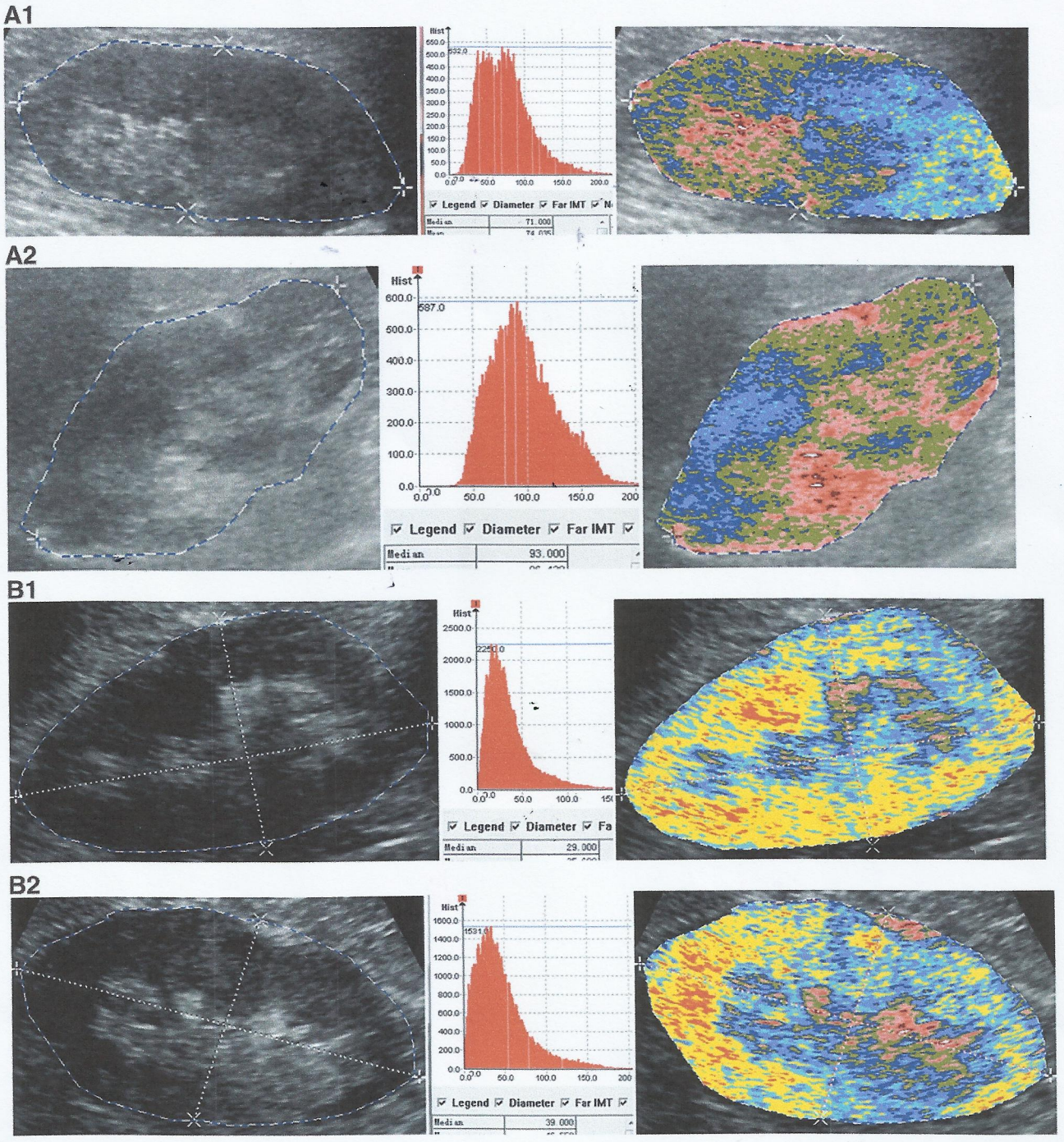

Figure 1

Examples of kidney echogenicity. Artificial colorization is achieved based on 14 intervals of brightness in gray-scale imaging. Different renal conditions yet to be investigated. (A) Unilateral to the renal artery stenosis, gray-scale median (GSM) = 71; contralateral to the stenosis, GSM = 93. (B) Unilateral to the renal artery stenosis, GSM = 29; contralateral to the stenosis, GSM = 39.

GSM did not correlate with kidney length or RI either for KIS + KCS, KIS, or KCS subgroups with coefficients equal to −0.32, −0.24, and −0.35 for length and 0.34, 0.43, and 0.35 for RI, respectively.

Summary

Echogenicity of kidneys in patients with unilateral renal artery stenosis, based on GSM measurements, was higher than for normal, young kidneys. Contralateral kidneys either had near-normal echogenicity or had the highest echogenicity of the subgroups analyzed. GSM was an independent variable uncorrelated with kidney length or flow resistivity index.

Discussion

This discovery level research was based on the assumption that tissue changes before symptoms appear and before kidney hemodynamics become abnormal. GSM noncorrelation with kidney lengths or flow RI indicated that echogenicity may indeed be an independent variable with additional information. This discussion focused on the adult findings. We will point out, however, that the percentage of children, 10% (2/0), in this research initial search, selected sequentially, was apparently very high. The reasons are beyond the scope of this manuscript but further investigation is warranted.

One expects that significant renal artery stenosis should, eventually, affect kidney tissue altering its echogenicity. One could ponder that the renal artery stenosis has yet to affect kidney tissue in some patients. Indeed, three of the adults included in this report had GSM within the normal-young range (27–48), and three more had GSM in a borderline region (49–53). We may assume, therefore, that renal artery stenosis affected the majority of ipsilateral kidneys (n = 12 or 67%). Further analysis not reported herein is suggestive that although echogenicity has increased in most patients, the resistivity index may still be within acceptable limits: another potential evidence that tissue changes before hemodynamics. These echogenic tissue changes are being ascribed to ischemia, and perhaps hypotension distal to the stenosis.

Another important question is what happens to the contralateral kidney. If the kidney ipsilateral to the stenosis is affected, one may presume that systemic alterations may occur. These systemic changes may influence the contralateral kidney. We have no evidence to ascribe the dramatic increase in echogenicity in eight (44%) kidneys contralateral to renal artery stenosis. These kidneys may have had other sources influencing hyperechogenicity. It is possible, however, that the supposedly unaffected kidney could be under systemic stress causing hyperechogenicity. The general conclusion, therefore, is that in some patients the contralateral kidney remains with near-normal echogenicity, while others were dramatically affected by the contralateral renal artery stenosis. In the latter cases, even the ipsilateral kidney was more affected.

Future research may expand USTC in the direction of regional evaluation of the kidney. This discovery level research was generic for the entire kidney. It could be applied as screening of tissue changes. Furthermore, the ability to quantitate renal conditions either as disease develops and progresses, or to monitor treatment might be possible. Comparison with pathology and clinical findings would be more complex than such simple quantitative monitoring application. Specific data on cortex, medulla, and pelvis, e g., might amplify the applications of this technique and warrants additional study.

In summary, GSM or echogenicity data may indicate if the ipsilateral kidney has tissue affected by the renal artery stenosis, and, if the contralateral kidney may also change its tissue due to the systemic influence of the stenosis.

References

1. Engelhorn ALDV, Engelhorn CA, Salles-Cunha SX. Initial evaluation of virtual histology ultrasonographic techniques applied to a case of renal transplant. *J Vasc Ultrasound* 2015;39:142–144.

2. Valiente Engelhorn AL, Engelhorn CA, Salles-Cunha SX, et al. Ultrasound tissue characterization of the normal kidney. *Ultrasound Q* 2012;28:275–280.

3. Menezes FH, Silveira TC, Silveira SAF, et al. Preliminary comparisons between in vivo ultrasonographic virtual histology and histopathological findings of endarterectomized carotid plaque. *J Vasc Bras* 2013;12:193–201.

4. Barros FS, Pontes SM, Prezotti BB, et al. Floating thrombus in the internal carotid artery: Surgical planning defined by vascular ultrasound. *Arq Bras Cardiol: Imagem Cardiovasc* 2013;26:335–340.

5. Salles-Cunha SX. Technical note: Ultrasonographic evaluation of aortic aneurysms treated with endoprosthesis. *J Vasc Bras* 2012;11:150–153.

6. Barros FS, Sandri JL, Prezotti BB, et al. Pulmonary embolism in a rare association to a floating thrombus detected by ultrasound in the basilic vein at the distal arm. *Rev Bras Ecocardiogr Imagem Cardiovasc* 2011;24:89–92.

7. Cassou-Birckholz MF, Engelhorn CA, Salles-Cunha SX, et al. Assessment of deep venous thrombosis by grayscale median analysis of ultrasound images. *Ultrasound Q* 2011;27:55–61.

8. Salles-Cunha SX. Duplex scanning for acute venous thrombosis. In: Peter Gloviczki, ed. *Handbook of Venous Disorders, Guidelines of the American Venous Forum*, 3rd ed. London, UK: Edward Arnold, Publisher; 2009:129–141.

9. Hashimoto H, Tagaya M, Niki H, et al. Computer-assisted analysis of heterogeneity on B-mode imaging predicts instability of asymptomatic carotid plaque. *Cerebrovasc Dis* 2009;28:357–364.

10. Marks NA, Ascher E, Hingorani AP, et al. Gray-scale median of the atherosclerotic plaque can predict success of lumen re-entry during subintimal femoral-popliteal angioplasty. *J Vasc Surg* 2008;47: 109–116.

11. Lal BK, Hobson RW II, Hameed M, et al. Noninvasive identification of the unstable carotid plaque. *Ann Vasc Surg* 2006;20:167–174.

12. Biasi GM, Froio A, Diethrich EB, et al. Carotid plaque echolucency increases the risk of stroke in carotid stenting: The imaging in carotid angioplasty and risk of stroke (ICAROS) study. *Circulation* 2004;110:756–762.

13. Lal BK, Hobson RW II, Pappas PJ, et al. Pixel distribution analysis of B-mode ultrasound scan images predicts histologic features of atherosclerotic carotid plaques. *J Vasc Surg* 2002;35:1210–1217.

14. Santos FTA, Rocha CA, Salles-Cunha SX, et al. Tissue characterization by photographic imaging during treatment of chronic venous ulcer: Technical note. *J Vasc Bras* 2015;14:177–181.

15. Pereira VHH, Costa Filho EM, Santos FTA, et al. Photographic image tissue characterization of the ulcerated diabetic foot during treatment: Technical note. *J Vasc Bras* 2013;12:303–307.

16. Polonio L, Prigol L, Camargo M, et al. Characterization of tissue by ultrasonography (CATUS) of transplanted kidneys: Discovery phase research. Presented at the Radiology Congress, Curitiba, PR, Brazil, September 2013.

17. Salles-Cunha SX, Silveira SAF. Chronic or mixed venous thrombosis? Ultrasonographic tissue characterization indicates presence

of segmental acute or subacute thrombosis. Presented at the 40th Congress of the Brazilian Society of Angiology and Vascular Surgery, Florianópolis, SC, September 30 to October 5, 2013.

18. Salles-Cunha SX, Silveira SAF. Ultrasonographic caracterização of deep venous thrombosis in lower extremities: Echogenicity increases with transducer compression. Poster presented at the 39th Society for Vascular Ultrasound Annual Meeting, Las Vegas, NV, July 15–18, 2015.

19. Salles-Cunha SX. Tissue characterization of cutaneous and subcutâneos compartments in aesthetic phlebology: Edema type differentiation. International Meeting on Aesthetic Phlebology (IMAP). Clube de Campo São Paulo, SP, March 13, 2015.

20. Salles-Cunha SX, Silveira SAF, Menezes FH. Case report: Ultrasound virtual histology to grade treatment of lower extremity lymphedema. Poster presented at the 36th Society for Vascular Ultrasound Annual Meeting, Washington, DC, June 7–9, 2012.

21. Salles-Cunha SX. Ultrasound virtual histology applied in the differentiation of lymphedema. Presented at the International Phlebology and Lymphology Meeting of Santos, SP, Brazil, August 11–13, 2011.

22. Abreu JAC, Salles Cunha SX, Pitta GBB, et al. Ultrasonographic tissue characterization post great saphenous vein treatment: Traditional stripping surgery versus laser thermal ablation. Presented at the 40th Congress of the Brazilian Society of Angiology and Vascular Surgery, Florianópolis, SC, September 30 to October 5, 2013.

23. Salles Cunha SX. Varjão de Oliveira, Guimaraes AF. Complementary role of thermography in the diagnosis of subclavian vein thrombosis: Case report. Poster presented at 40th Congress of the Brazilian Society of Angiology and Vascular Surgery, Florianópolis, SC, September 30 to October 5, 2013.

24. Salles Cunha SX. Varjão de Oliveira. Thermography complements arterial ultrasonography and pressure measurements in case of neurovascular isquemia of a painful diabetic foot. Poster presented at 40th Congress of the Brazilian Society of Angiology and Vascular Surgery, Florianópolis, SC, September 30 to October 5, 2013.

25. Oliveira HV, Salles-Cunha SX. Digital traumatic fistula and arteriovenous malformation in patient with ulnar nerve compression syndrome. Oral case presentation at the 39th Society for Vascular Ultrasound Annual Meeting, Las Vegas, NV, July 15–18, 2015.

26. Beach KW, Paun M, Primozich JF. Principles and instruments of diagnostic ultrasound and doppler ultrasound. In: Aburahma AF, Bergan JJ (eds.). *Noninvasive Vascular Diagnosis: A Practical Guide to Therapy*, 2nd ed. London: Springer-Verlag; 2007:27.

27. Professonal Guidelines Subcommittee. Vascular technology professional performance guidelines: Renal artery duplex imaging. Society for Vascular Ultrasound. Available at: http://www.svunet.org/practicemanagementmain/professionalperformanceguidelines., 2014.

28. Engelhorn AL, Engelhorn CA. Vascular ultrasonography for renal artery evaluation. In: Engelhorn AL, Morais Filho D, Barros FS, Coelho NA and Engelhorn CA (eds.). *Vascular ultrasonography: Practical guide*. Guia prático de ultrasonografia vascular, 3rd e Rio de Janeiro, RJ, Brazil: DiLivros, Publ.; 2016;207–223.

29. Pemble L, Gibbs H. The findings of a retrospective audit of clinical indications and outcomes related to renal artery duplex ultrasounds performed during a 2-year period. *J Vasc Ultrasound* 2012;36:13–18.

30. Lee ES, DelPizzo D, Murray K, et al. Predictors of a technically limited renal artery duplex study: A retrospective analysis. *J Vasc Ultrasound* 2009;33:181–183.

31. Coombs P. Color duplex of the renal arteries: Diagnostic criteria and anatomical windows for visualization. *J Vasc Ultrasound* 2004;28: 89–95.

32. Guzman RP, Isaacson JA, Zierler RE, et al. End-diastolic rations from the renal artery and kidney in patients with and without proximal renal artery stenosis. *J Vasc Technol* 1996;20:77–80.

33. Staub D, Canevascini R, Huegli RW, et al. Best duplex-sonographic criteria for the assessment of renal artery stenosis–correlation with intra-arterial pressure gradient. *Ultraschall Med* 2007;28:45–51.

34. Poe PA. Color duplex ultrasound evaluation of renal and mesenteric arteries. *J Vasc Ultrasound* 2005;29:149–155.

35. Engelhorn CA, Engelhorn ALDV, Cassou MF. Renal artery stenosis: Need for validation of diagnostic criteria in the vascular laboratory. *J Vasc Bras* 2005;4:243–248.

36. Strandness DE Jr. Duplex imaging for the detection of renal artery stenosis. *Am J Kidney Dis* 1994;24:674–678.

37. AbuRahma AF, Srivastava M, Mousa AY, et al. Critical analysis of renal duplex ultrasound parameters in detecting significant renal artery stenosis. *J Vasc Surg* 2012;56:1052–1059.

38. Neumyer MM. Characterization of blood flow patterns in the hepatoportal, mesenteric and renal vessels by analyzing doppler spectral waveforms. *J Vasc Ultrasound* 2012;36:113–122.

39. Isaacson JA, Zierler RF, Spittell PC, et al. Noninvasive screening for renal artery stenosis: Comparison of renal artery and renal hilar duplex scanning. *J Vasc Technol* 1995;19:105–110.

40. Louis J, Isaacson JA, Zierler RE, et al. Hemodynamic parameters for diagnosis of advanced renal artery stenosis by duplex ultrasound. *J Vasc Technol* 1994;18:61–66.

41. Isaacson JA, Zierler RE, Bergelin RO, et al. A method for minimizing variability in kidney length measurements during renal artery duplex scanning. *J Vasc Technol* 1994;18:23–27.